Geomechanics and Engineering, *Vol. 11, No. 6 (2016) 787-803*
DOI: http://dx.doi.org/10.12989/gae.2016.11.6.787

New reinforcement algorithms in discontinuous deformation analysis for rock failure

Yunjuan Chen [*1], Weishen Zhu [2], Shucai Li [2] and Xin Zhang [1]

[1] *Shandong Provincial Key Laboratory of Appraisal and Retrofitting in Building Structures, Shandong Jianzhu University, Ji'nan 250101, Shandong, China*
[2] *Geotechnical and Structural Engineering Research Center, Shandong University, Ji'nan 250061, Shandong, China*

(*Received October 26, 2015, Revised May 29, 2016, Accepted July 29, 2016*)

Abstract. DDARF (Discontinuous Deformation Analysis for Rock Failure) is a numerical algorithm for simulating jointed rock masses' discontinuous deformation. While its reinforcement simulation is only limited to end-anchorage bolt, which is assumed to be a linear spring simply. Here, several new reinforcement modes in DDARF are proposed, including lining reinforcement, full-length anchorage bolt and equivalent reinforcement. In the numerical simulation, lining part is assigned higher mechanical strength than surrounding rock masses, it may include multiple virtual joints or not, depending on projects. There must be no embedding or stretching between lining blocks and surrounding blocks. To realize simulation of the full-length anchorage bolt, at every discontinuity passed through the bolt, a set of normal and tangential spring needs to be added along the bolt's axial and tangential direction. Thus, bolt's axial force, shearing force and full-length anchorage effect are all realized synchronously. And, failure criterions of anchorage effect are established for different failure modes. In the meantime, from the perspective of improving surrounding rock masses' overall strength, a new equivalent and tentative simulation method is proposed, it can save calculation storage and improve efficiency. Along the text, simulation algorithms and applications of these new reinforcement modes in DDARF are given.

Keywords: DDARF; lining reinforcement; full-length anchorage bolt; failure criterion; equivalent reinforcement

1. Introduction

Discontinuous Deformation Analysis method (DDA) is originally proposed by Shi G.H. and Goodman in the early 1980s, its research object is block system, cutby random joints or faults. Blocks can be arbitrarily shaped, while their motions must obey Newton's Theorem. There are three contacting relations between blocks, such as angle-angle contact, angle-edge contact and edge-edge contact. Blocks' motions and contacts are unified into equations by the principle of minimum potential energy (Shi 1988, 1993, 1999, Ma *et al*. 2010). DDA meets the elastic theory and it is as rigorous as FEM. Besides, it can simulate large displacements as DEM (Zhu *et al*. 2014, He *et al*. 2014).

Based on the DDA framework, a new numerical method——Discontinuous Deformation

*Corresponding author, Ph.D., E-mail: skdcyj@126.com

 ISSN: 2005-307X (Print), 2092-6219 (Online)

Analysis for Rock Failure (DDARF) is presented (Jiao *et al*. 2012). It not only has the:

(i) Triangular blocks

Network of random joints in DDARF is generated by Monte-carlo method. Based on the network, calculation model will be divided into multiple triangular blocks. While, prior to this block division, there are several preparatory works need to be done, one is that partitioning the research object into multiple single-connected domains; and the other is that generating triangular blocks in each sub-domain, and at last combining all blocks.

(ii) Simulation on materials' non-uniform parameters

Calculation model is composed of lots of triangular blocks, and their mechanical parameters are non-uniform. It is planned to be realized by Wei-bull distribution. Assuming that the model has n blocks, first of all, generating random digits ξ_i of uniform distribution at interval [0,1] using the linear congruence method (Eq. (1a)); secondly, using the direct sampling method, mechanical parameters η_i of Wei-bull distribution can be gotten based on those random digits ξ_i (Eq. (1b)).

$$\phi(\eta_i) = \xi_i \tag{1a}$$

$$\eta_i = \beta_0[-In(1-\xi_i)]^{\frac{1}{h}} \tag{1b}$$

where β_0 is average value of materials' parameters.

(iii) Changes from virtual joints to real joints

During the block division process, a large number of block boundaries will be generated and defined as virtual joints, they provide possible ways for crack expansion. Mohr-Coulomb criterion and the maximum tensile stress criterion are used to judge joints' dynamic variations, when a virtual joint reaches its ultimate strength, that is to say, if the virtual joint's strength obeys Mohr-Coulomb criterion or the maximum tensile stress criterion, it will be turned into real joint and its mechanical parameters are also reduced accordingly (Jiao *et al*. 2014).

Combining DDA's general characteristics and its own three unique properties, DDARF can successfully simulate the whole process of crack initiation, propagation, coalescence, and crushing for intermittent jointed rock masses.

Although DDARF has developed rapidly, yet its reinforcement simulation is only limited to end-anchorage bolt, which is assumed to be a linear spring, obeying Hooke Law. It only has the ability to simulate bolt's axial force and neglects bolt's shearing force, which is far from actual projects. As a consequence, it is necessary to explore new reinforcement algorithms in DDARF. At home and abroad, many scholars have attempted to study the improvement and development of reinforcement simulations for discontinuous deformation analysis. Ke (1997) put forward a new bolt model in 1990s, to overcome drawback that the original algorithm can't simulate bolt's shearing force, and it achieved satisfactory results. Zheng (2010) and Wu (2003) proposed to add springs at each discontinuity passed through a bolt, to simulate the full-length anchorage effect. While, this method should know all directions of discontinuities passed through this bolt in advance. For regular joints, it may be easier, nevertheless, if model's joints are numerous and random, it will become complex. Those published reinforcement researches are mainly confined to

DDA, and by now there is few related to DDARF.

In this paper, several kinds of reinforcement modes commonly used in rock engineering will be proposed, including lining reinforcement, bolt reinforcement and equivalent reinforcement, their numerical algorithms in DDARF will also be given. For bolt reinforcement, it not only refers to end-anchorage bolt, but also to full-length anchorage bolt, and the latter can consider bolt's axial force and shearing force simultaneously. The remainder of this paper is organized as follows. Section 2 illustrates numerical algorithm of lining reinforcement in DDARF. Section 3 discusses the reinforcement mechanism and effect of full-length anchorage bolt. Section 4 carries out a new thinking of equivalent reinforcement and reviews its simulation effect in rock engineering. Finally, concluding remarks are listed in Section 5.

2. Liningreinforcement

Lining is a structure built along tunnel periphery with certain thickness, mainly to prevent deformation or collapse of rock masses, it is widely used in rock engineering (Ngoc *et al*. 2014). Herein, its simulation uses the coupled modeling program of DDARF and AutoCAD. AutoCAD has powerful drawing functions and visualized operation interface, it is easier to be grasped, and also it can offer the Object-ARX (Noel *et al*. 1995), a secondary development tool. .ARX file can be generated in VC++ compile environment and it can use all the drawing commands of AutoCAD. Procedures of establishing calculation model by this method are as follows: (i) loading the .ARX file into AutoCAD; (ii) plotting the geometrical figures in AutoCAD using its drawing commands; (iii) selecting the drawing figures, and converting it to be calculation model of DDARF.

Drawing model in AutoCAD is shown in Fig. 1. Take a tunnel as an example, lining part can be built as one block or more according to projects. By adding virtual joints, lining part would be divided into multiple triangular blocks. Contacts between lining blocks and surrounding blocks should obey the kinematic conditions of no embedding or no stretching, as same as around rock mass parts. Imported calculation model in DDARF is given in Fig. 2.

Usually, mechanical strength of lining parts should be higher than surrounding rock masses, and its stress-strain curve is mainly elastic-brittle or elastic-plastic. However, as a new numerical

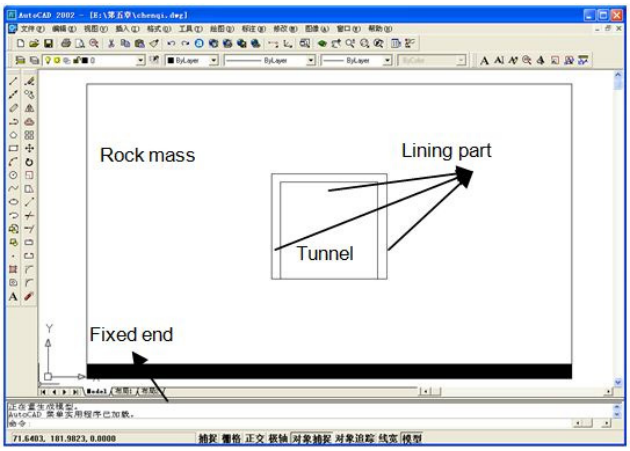

Fig. 1 Calculation model with lining reinforcement in AutoCAD

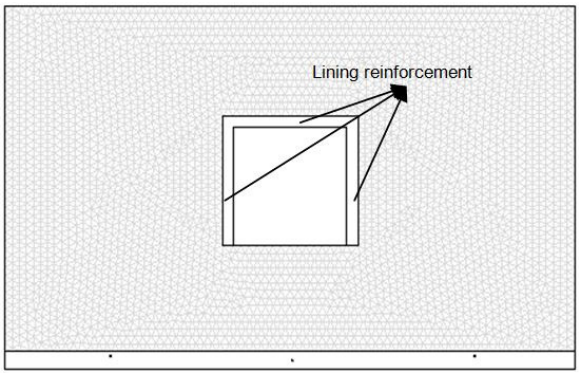

Fig. 2 Imported calculation model with lining reinforcement in DDARF

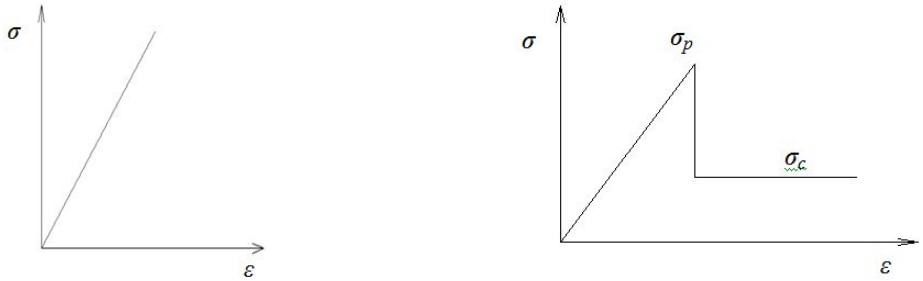

(a) Linear elastic constitutive model (b) Elastic-brittle constitutive model

Fig. 3 Stress-strain curves of different constitutive models

method, DDARF only gives algorithms for linear elastic constitutive model (seen in Fig. 3(a)). Here, to ensure the simulation accuracy of lining reinforcement, we will study the elastic-brittle lgorithms for (Nikolic *et al*. 2015, Tateki *et al*. 2006, Li *et al*. 2014) lining's constitutive model seen in Fig. 3(b)) in DDARF.

Block's stress state is judged by Mohr-Coulomb criterion and the maximum tensile stress criterion. When $F < 0$, block will keep the linear elastic characteristics; while, when $F = 0$, block will enter the post-peak period (Mohammadi and Tavakoli 2015) and its mechanical strength will decrease accordingly. Mohr-Coulomb criterion and the maximum tensile stress criterion can be expressed in DDARF as Eqs. (2) and (3).

$$F^s = 2\sqrt{\left(\frac{\sigma_x - \sigma_y}{2}\right)^2 + {\tau_{xy}}^2} - \left(\sigma_x + \sigma_y\right)\sin\varphi - 2c\cos\varphi \tag{2}$$

where σ_x and σ_y are the principle stress along x and y direction, respectively. τ_{xy} is the shearing force, c is cohesion and ϕ is the friction angle.

$$\Pi_e = \frac{1}{2}\iint (\varepsilon_x \quad \varepsilon_y \quad \gamma_{xy})\mathbf{E_i}\begin{pmatrix}\varepsilon_x\\ \varepsilon_y\\ \gamma_{xy}\end{pmatrix} dxdy \tag{3}$$

$$\begin{aligned} &= \frac{1}{2}\mathbf{D}_\mathbf{i}^{\mathrm{T}}\left(\iint \mathbf{E}_\mathbf{i} dxdy\right)\mathbf{D}_\mathbf{i} \\ &= \frac{S}{2}\mathbf{D}_\mathbf{i}{}^{\mathrm{T}}\mathbf{E}_\mathbf{i}\mathbf{D}_\mathbf{i} \end{aligned} \tag{3}$$

where σ_t is the tensile strength of rock masses.

When $F < 0$, blocks keep at the linear elastic stage. For underground cavern engineering such as dams or tunnels, deformations won't occur along their axial direction because of the structural restriction, it belongs to plane strain problem, and then block's elastic strain energy can be expressed as Eq. (4).

$$\begin{aligned} \Pi_e &= \frac{1}{2}\iint (\varepsilon_x \quad \varepsilon_y \quad \gamma_{xy})\mathbf{E}_\mathbf{i}\begin{pmatrix}\varepsilon_x\\ \varepsilon_y\\ \gamma_{xy}\end{pmatrix} dxdy \\ &= \frac{1}{2}\mathbf{D}_\mathbf{i}^{\mathrm{T}}\left(\iint \mathbf{E}_\mathbf{i} dxdy\right)\mathbf{D}_\mathbf{i} \\ &= \frac{S}{2}\mathbf{D}_\mathbf{i}{}^{\mathrm{T}}\mathbf{E}_\mathbf{i}\mathbf{D}_\mathbf{i} \end{aligned} \tag{4}$$

where S is block's area.

Contributions to overall equations can be obtained as Eq. (5).

$$S\mathbf{E}_\mathbf{i} \rightarrow \mathbf{K}_{\mathbf{ii}} \tag{5}$$

Once $F = 0$, block's stress will decrease rapidly to the residual stress σ^c (σ_x^c σ_y^c τ_{xy}). Assuming σ^c = (0 0 0 σ_x^c σ_y^c τ_{xy}) and ε^p = (0 0 0 ε_x^p ε_y^p γ_{xy}^p), then the strain energy is expressed as Eq. (6).

$$\begin{aligned} \Pi_{\sigma^c} &= \iint[(\varepsilon_x - \varepsilon^p{}_x)\sigma^c{}_x + (\varepsilon_y - \varepsilon^p{}_y)\sigma^c{}_y + (\gamma_{xy} - \gamma^p{}_{xy})\tau^c{}_{xy}]dxdy \\ &= S[(\varepsilon_x - \varepsilon^p{}_x)\sigma^c{}_x + (\varepsilon_y - \varepsilon^p{}_y)\sigma^c{}_y + (\gamma_{xy} - \gamma^p{}_{xy})\tau^c{}_{xy}] \end{aligned} \tag{6}$$

with contributions to overall equations

$$-S\boldsymbol{\sigma}_\mathbf{c} \rightarrow \mathbf{F}_\mathbf{i} \tag{7}$$

where ε^p denotes block's peak strain.

Simulations on elastic-brittle constitutive model in DDARF can be realized by compiling Eq. (5) and (7), at the same time, block's stress-strain relationship should be updated.

3. Full-length anchorage bolt

3.1 Simulation on end-anchorage bolt in DDARF

In original DDARF, bolt is assumed to be a linear spring connecting point (x_1 y_1) in block i and point (x_2 y_2) in block j, its reinforcement form is end-anchorage and plotted in Fig. 4.

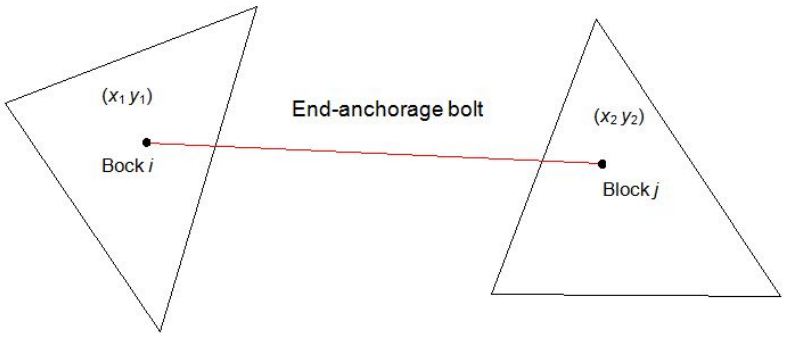

Fig. 4 End-anchorage bolt

Length of end-anchorage bolt can be expressed as Eq. (8).

$$l = \sqrt{(x_1 - x_2)^2 + (y_1 - y_2)^2} \tag{8a}$$

with

$$l_x = \frac{x_1 - x_2}{l} \tag{8b}$$

$$l_y = \frac{y_1 - y_2}{l} \tag{8c}$$

where l_x and l_y are the direction cosine along x and y directions of bolt, respectively.

Elongation of end-anchorage bolt can be calculated as Eq. (9).

$$\begin{aligned} dl &= \begin{pmatrix} u_1 & \upsilon_1 \end{pmatrix} \begin{pmatrix} l_x \\ l_y \end{pmatrix} - \begin{pmatrix} u_2 & \upsilon_2 \end{pmatrix} \begin{pmatrix} l_x \\ l_y \end{pmatrix} \\ &= \mathbf{D_i^T T_i^T} \begin{pmatrix} l_x \\ l_y \end{pmatrix} - \mathbf{D_j^T T_j^T} \begin{pmatrix} l_x \\ l_y \end{pmatrix} \end{aligned} \tag{9}$$

Taking into account the initial force such as pre-stress, there will be initial elongation along the axial direction of bolt, and it can be denoted as δ_m. Thus, strain energy Π_e of end-anchorage bolt is gotten as Eq. (10).

$$\Pi_{ij} = \frac{k_b}{2}(\delta_m + dl)^2 = \frac{k_b}{2}(\delta_m + [D_j]^T[G_j] - [D_i]^T[E_i])^2 \tag{10}$$

where k_b is the axial rigidity of bolt.

with contributions to overall equations

$$\begin{aligned} k_b[E_i][E_i]^T &\to [K_{ii}], \quad & k_b[G_j][G_j]^T &\to [K_{jj}] \\ -k_b[E_i][G_j]^T &\to [K_{ij}], \quad & -k_b[G_j][E_i]^T &\to [K_{ji}] \end{aligned} \tag{11}$$

$$-k_b\delta_m[E_i]\rightarrow[F_i],\qquad k_b\delta_m[G_j]\rightarrow[F_j] \tag{11}$$

Take f_0/k_b replace of δ_m, and then the strain energy Π_e of pre-stressed bolt becomes as Eq. (12).

$$\Pi_{ij}=\frac{k_b}{2}(\frac{f_0}{k_b}+dl)^2 \tag{12}$$

with contributions to overall equations

$$\begin{aligned} &k_b[E_i][E_i]^T\rightarrow[K_{ii}], && k_b[G_j][G_j]^T\rightarrow[K_{jj}]\\ &-k_b[E_i][G_j]^T\rightarrow[K_{ij}], && -k_b[G_j][E_i]^T\rightarrow[K_{ji}]\\ &-f_0[E_i]^T\rightarrow[F_i], && f_0[G_j]^T\rightarrow[F_j] \end{aligned} \tag{13}$$

3.2 Simulation on full-length anchorage bolt in DDARF

3.2.1 Simulation mechanism of full-length anchorage bolt in DDARF

Assuming that deformations of rock masses are mostly produced because of discontinuities, when a bolt passes through discontinuities, their motions along bolt's axial and normal directions will both be constrained. Decompose the restrained force in two directions, one is along bolt's axial direction and the other is along bolt's normal direction, and add a set of springs along these two directions in order to simulate bolt's axial force and shearing force in DDARF (Chen *et al*. 2014). The full-length anchorage bolt is drawn in Fig. 5. Advantage of this decomposing method is that it doesn't need to compute every discontinuity's orientation in advance and then can improve the computational efficiency.

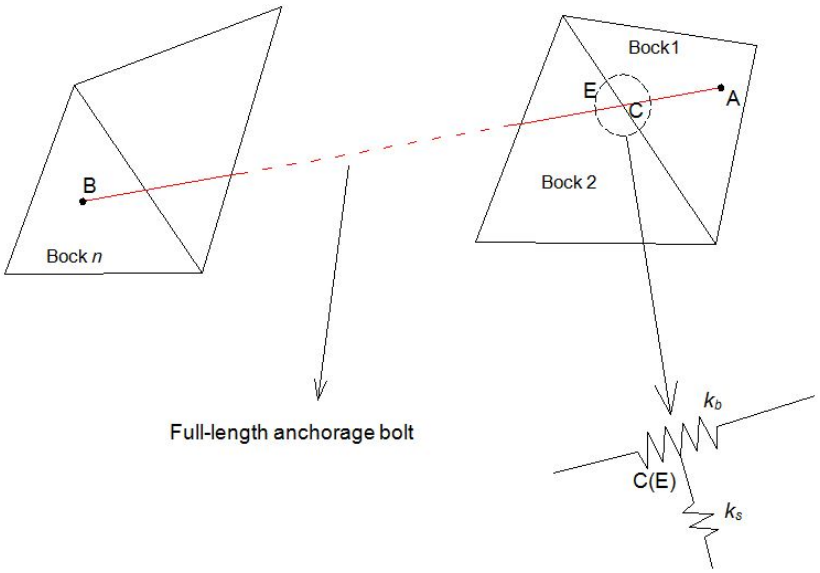

Fig. 5 Full-length anchorage bolt

At every discontinuity, simulation on the axial restriction of full-length anchorage bolt is as same as that of end-anchorage bolt. The axial elongation of full-length anchorage bolt is expressed as Eq. (14).

$$\begin{aligned} dl &= \begin{pmatrix} u_1 & \upsilon_1 \end{pmatrix} \begin{pmatrix} l_x \\ l_y \end{pmatrix} - \begin{pmatrix} u_2 & \upsilon_2 \end{pmatrix} \begin{pmatrix} l_x \\ l_y \end{pmatrix} \\ &= \mathbf{D_i^T T_i^T} \begin{pmatrix} l_x \\ l_y \end{pmatrix} - \mathbf{D_j^T T_j^T} \begin{pmatrix} l_x \\ l_y \end{pmatrix} \end{aligned} \tag{14}$$

axial strain energy (including initial elongation δ_m) is expressed as Eq. (15).

$$\Pi_{ij} = \frac{k_b}{2} (\delta_m + \left[D_j \right]^T \left[G_j \right] - \left[D_i \right]^T \left[E_i \right])^2 \tag{15}$$

with contributions to overall equations

$$\begin{aligned} &k_b \left[E_i \right] \left[E_i \right]^T \to \left[K_{ii} \right], \quad && k_b \left[G_j \right] \left[G_j \right]^T \to \left[K_{jj} \right] \\ &-k_b \left[E_i \right] \left[G_j \right]^T \to \left[K_{ij} \right], \quad && -k_b \left[G_j \right] \left[E_i \right]^T \to \left[K_{ji} \right] \\ &-k_b \delta_m \left[E_i \right] \to \left[F_i \right], \quad && k_b \delta_m \left[G_j \right] \to \left[F_j \right] \end{aligned} \tag{16}$$

or (take f_0 / k_b replace of δ_m)

$$\begin{aligned} &k_b \left[E_i \right] \left[E_i \right]^T \to \left[K_{ii} \right], \quad && k_b \left[G_j \right] \left[G_j \right]^T \to \left[K_{jj} \right] \\ &-k_b \left[E_i \right] \left[G_j \right]^T \to \left[K_{ij} \right], \quad && -k_b \left[G_j \right] \left[E_i \right]^T \to \left[K_{ji} \right] \\ &-f_0 \left[E_i \right]^T \to \left[F_i \right], \quad && f_0 \left[G_j \right]^T \to \left[F_j \right] \end{aligned} \tag{17}$$

where f_0 is the full-length anchorage bolt's pre-stress.

The following analysis will be mainly focused on bolt's tangential constraints. At each discontinuity, supposing the intersection points are point $C(x_i\ y_i)$ of block 1 and point $E(x_j\ y_j)$ of block 2, these two points' relative displacements can be expressed as Eq. (18).

$$dl = [T_j][D_j] - [T_i][D_i] \tag{18}$$

with its axial component

$$dl^n = \left([T_j][D_j] - [T_i][D_i] \right)^T \begin{pmatrix} l_x \\ l_y \end{pmatrix} \tag{19}$$

and the tangential displacement can be obtained by Eq. (20).

$$dl^s = \sqrt{dl^2 - (dl^n)^2} \tag{20}$$

Tangential strain energy of the full-length anchorage bolt is obtained as Eq. (21).

$$\Pi_s = k_s[dl^2 - (dl^n)^2]/2 \tag{21}$$

with contributions to overall equations

$$\left.\begin{aligned} & k_s[T_i]^T[T_i] - k_s[E_i][E_i]^T \rightarrow [K_{ii}] \\ & k_s[T_j]^T[T_j] - k_s[G_j][G_j]^T \rightarrow [K_{jj}] \\ & -k_s[T_i]^T[T_j] + k_s[E_i][G_j]^T \rightarrow [K_{ij}] \\ & -k_s[T_j]^T[T_i] + k_s[G_j][E_i]^T \rightarrow [K_{ji}] \end{aligned}\right\} \tag{22}$$

Combining Eqs. (16) and (22) or combining Eqs. (17) and (22), we will get the total contributions of full-length anchorage bolt. And then, simulation on reinforcement effect of the full-length anchorage bolt will be realized in DDARF.

3.2.2 Engineering application of full-length anchorage bolt in DDARF

A highway tunnel's surrounding rock is rich in joints, and there are three groups of intermittent joints. Joint space follows fixed-distribution, joint length follows normal-distribution and joint angle follows exponential-distribution, their geometrical information is described in Table 1. Numerical model's size is 100 m × 80 m (width × height), its depth is 270 m and size of the tunnel's cross section is 8 m × 7 m (span × height). Vertical force focused on model is mainly rock masses' gravity, the lateral pressure coefficient is 1.3. Model's numerical parameters are shown in Table 2.

Discontinuous deformation analysis on surrounding rock masses' stabilities of this tunnel is studied by DDARF. To keep in line with the actual rock engineering and consider surrounding rock masses' stress release, bolts are added to rock masses after tunnel excavation. Here, two bolt reinforcement modes are taken, one with end-anchorage bolt and the other with full-length

Table 1 Geometrical parameters of model's random joints

Joints	Space /m	Length /m		Angle /(°)
		Mean value	Square error	
1	4	5	0.5	50
2	3	5	0.5	120
3	3.5	5	0.2	80

Table 2 Mechanical parameters of numerical model

Classes	Density /(g/cm^3)	Elastic modulus /GPa	Poisson's ratio	Friction angle /(°)	Cohesion /MPa	Tensile strength /MPa
Rock mass	2.6	40	0.28	36	5	5
Virtual joint	-	-	-	36	5	5
Real joint	-	-	-	33	4	0

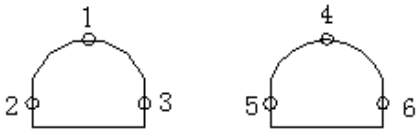

Fig. 6 Measuring points of highway tunnel

anchorage bolt. Bolt length is 2m, bolt space is 0.8m, the axial stiffness is 22000KN/m and the tangential stiffness is 10000 KN/m. Compared to end-anchorage bolt, it needs to input coordinate parameters of points pass through the full-length anchorage bolt in every discontinuity. Take vaults' midpoints and sidewalls' midpoints as the measuring points, plotted in Fig. 6.

After this highway tunnels' excavation, crack expansion of surrounding rock mass in DDARF are shown in Fig. 7 and displacements of measuring points are demonstrated in Fig. 8.

As it can be observed, reinforcement effect of the full-length anchorage bolt is better than end-anchorage bolt, expanded cracks' quantities and scales of surrounding rock mass are restricted obviously, especially the arch of right tunnel, where the displacement is reduced by 20.2%. From the point of crack expansion and displacements, we can see that the full-length anchorage bolt can well control surrounding rock masses' deformation, compared to end-anchorage bolt.

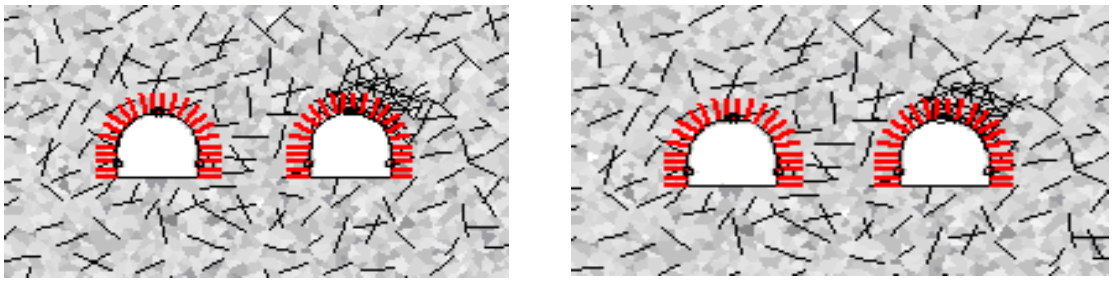

(a) End-anchorage bolt reinforcement (b) Full-length anchorage bolt reinforcement

Fig. 7 Crack expansion of highway tunnels' surrounding rock mass

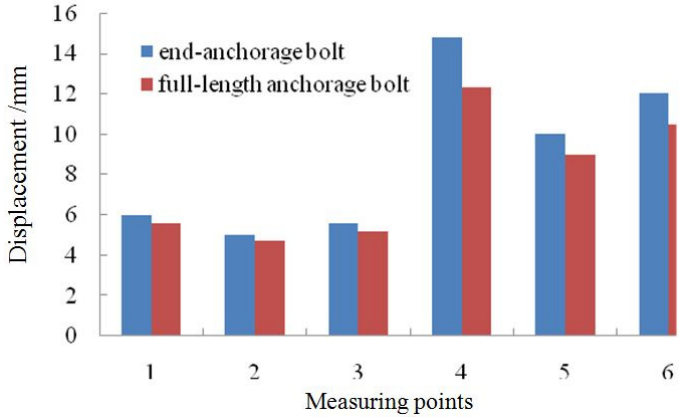

Fig. 8 Measuring points' displacements of surrounding rock mass

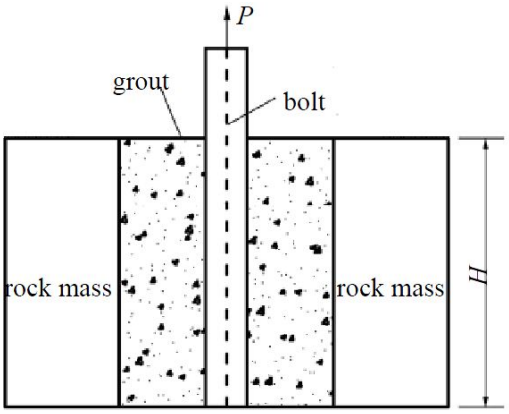

Fig. 9 Reinforcement of bolt to rock mass

3.3 Judgment on anchorage failure in DDARF

As an important support mode in rock engineering, bolt can reinforce rock mass well, as shown in Fig. 9.

There are usually four anchorage failure modes in rock engineering, including broken of bolt, slippage between bolt and grout, slippage between grout and surrounding rock mass, as well as the total failure of surrounding rock mass such as cone destruction. Herein, in view of the most common failure modes (bolt's broken and slippage) in rock engineering, we adopt corresponding failure criterions (Li *et al*. 2013) in DDARF:

(i) Anchorage failure of bolt's broken

A bolt will be broken when pulling force reaches its ultimate strength, and then the anchorage effect will fail. To this failure mode, it is suggested to use the maximum tensile stress criterion

$$\sigma_{\max} \le \sigma_t \tag{23}$$

where $\sigma_{\max}$ is the maximum pulling force focused on bolt and σ_t is the ultimate strength of bolt.

(ii) Anchorage failure of slippage

The slippage failure usually occurs between bolt and grout or between grout and surrounding rock masses, they both can be simply expressed as that the grout reaches its ultimate state, and then leading the slippage, it is deemed to be one-off and neglects the progressive failure process. Take grout as the research object, Mohr-Coulomb criterion is suggested here to judge whether the grout reaches its ultimate state or not

$$\tau_{xy} = \sqrt{\frac{(\sigma_x + \sigma_y)^2 \sin^2\phi}{4} + \frac{c(\sigma_x + \sigma_y)\sin 2\phi}{2} + c^2\cos^2\phi - \frac{(\sigma_x - \sigma_y)^2}{4}} \tag{24}$$

Neither of these two failure criterions has the priority, any one which bolt's stress state obeys firstly, it will work and decide the failure modes. In order to valid the effectiveness of these above failure criterions, DDARF simulation is done according to a laboratory test (Zhao 2009): the

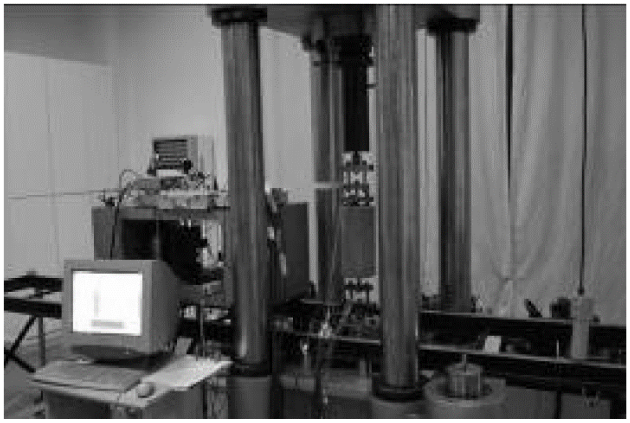

Fig. 10 RLJW-2000 pull-out test system

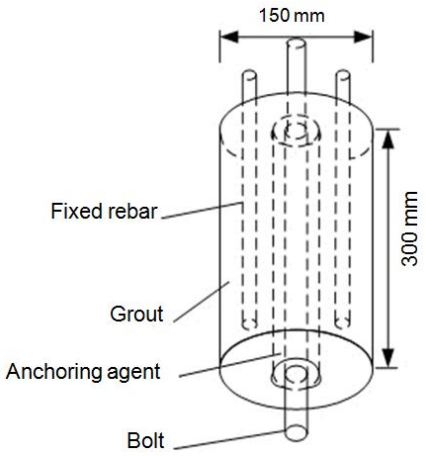

Fig. 11 Diagram of pull-out specimen

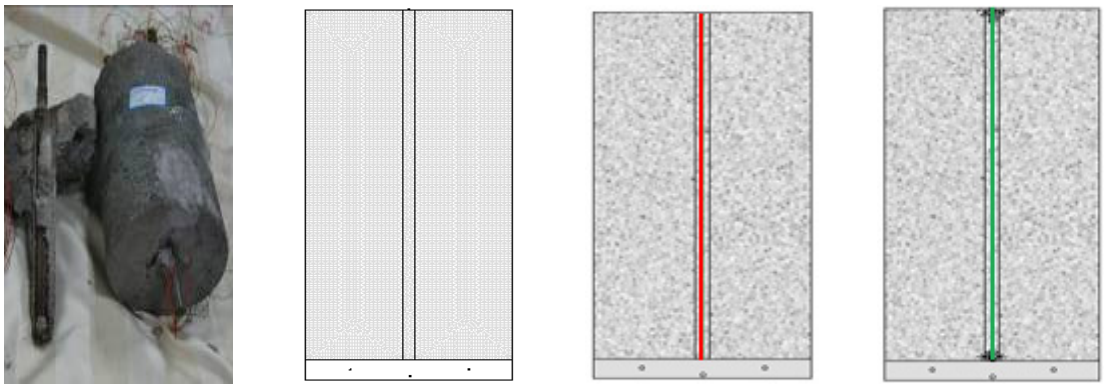

(a) Laboratory test (b) Numerical model (c) Before failure (d) Slippage failure

Fig. 12 Comparison of numerical simulation with laboratory test

specimen is made of C20 grout, its elastic modulus is 10 GPa and poisson's ratio is 0.25, bolt's elastic modulus is 200 GPa, and the pull-out test is done with RLJW-2000 testing machine, seen in Fig. 10. Specimen is fixed at the top by rebar and the pulling force focuses on the bottom, shown in Fig. 11. In DDARF, bolt's color is firstly set to be red, in order to consist with the original program. Then, when the reinforcement effect fails, bolt's color will become accordingly. If bolt's broken failure appears, it will become yellow and if slippage failure appears, it will become green.

In the laboratory test, when the pulling force reaches 10KN, bolt is pulled out and the anchorage effect fails. Take the same physical and mechanical parameters as those of the test, numerical simulation is done and the result shows that, when the pulling force reaches 10 KN, the bolt's color becomes green, which illustrates that the anchorage effect fails owing to slippage, as shown in Fig. 12.

Result in Fig. 12 shows that, judgment on anchorage failure in DDARF is more accurate, well in agreement with the laboratory test. Changes of bolt's color can reflect the anchorage failure modes, based on which, it has the ability to offer warning for anchorage safety in rock engineering, and then guide further designs for parts weaker or easier to fail.

4. Equivalent reinforcement

4.1 Mechanism of equivalent reinforcement in DDARF

Reinforcement effect in rock engineering is very complicated, while, in the final analysis, they all can be considered to improve rock masses' force-bearing capacity and mechanical strength. In other words, reinforcement effect can be reflected by the increase of surrounding rock masses' mechanical strength.

In a large underground engineering, there may be up to tens of thousands of bolts, their numerical simulations need to consume a large amount of computation time. And, if the software alone is not a good grasp of bolt's load-transfer mechanism, then the simulation effect would be non-ideal. Therefore, for a relatively newer software such as DDARF, it may be more appropriate to simulate the reinforcement effect from equivalent perspective.

Zhu W.S. has studied the equivalent mechanical parameters of reinforced rock masses through a large number of tests (Zhu and Zhang 1994), and shows that, the increased effects on strength and stiffness for rock masses are much larger than other additional effects, empirical formula of reinforced rock masses given by him is shown in Eq. (25). Although this formula cannot applicable to all rock masses, yet it covers most common cases, or to say it has great reference value for most reinforced rock masses. Herein, we will use the empirical formula to study equivalent reinforcement in DDARF.

$$\begin{cases} c_1 = c_0 + \eta \dfrac{\tau s}{ab} \\ \varphi_1 = \varphi_0 \end{cases} \tag{25}$$

where, c_0 and φ_0 are cohesion and friction angel of rock masses before support, respectively. c_1 and φ_1 are cohesion and friction angel of rock masses after support, respectively. τ and s are bolt's shearing strength and cross area. a and b are bolt's vertical and horizontal spacing, and η is generally valued in the range of 2 ~ 5, related to factors such as bolt's diameter, etc.

4.2 Engineering application of equivalent reinforcement in DDARF

Yi'meng hydro-power station is located in Fei county, Lin'yi city of China, its pivotal projects include channel system, reservoir system and underground powerhouse system, etc. Surrounding rock masses are given priority to granodiorite and gneissic diorite, they are mainly breezed and belong to class II and class III, local parts with faults or fractures belong to class IV and class V. The underground powerhouse system is deep in 385m or so, it includes main workshop, main transformer room, tail room, busbar cave, tailrace tunnel, etc. The main workshop's excavation size is 166 m × 25.5 m × 53 m (length × span × height) and its excavation elevation of top arch is 155.5m. Main transformer room's excavation size is 145 m × 21 m × 22 m (length × span × height). Tail room's excavation size is 118.5 m × 10 m × 34.4 m (length × span × height), and the busbar cave's excavation size is 40 m × 8.5 m × 9.5 m (length × span × height). Three-dimensional numerical model of this hydro-power station is established by FEM (shown in Fig. 13), in order to get the side pressure coefficient. In numerical calculation, inversion analysis method of in-situ stresses is adopted and the side pressure coefficient is computed to be 0.98.

Because faults cross through main workshop and tail room in unit 1#, so take unit 1# as the research object in DDARF. In the numerical simulation, influences of faults f10, f13, f61, f62, f63 and f64 on surrounding rock masses' stabilities are taken into account. According to the engineering background and numerical experience, η is assumed to be 3.5. Three numerical schemes are analyzed: (1) excavation without bolt; (2) excavation with full-length anchorage bolt (Main workshop: diameter of 28 mm, length of 6/9 m, spacing is 1.5 m; Main transformer room and Tail room: diameter of 25 mm, length of 5/7 m, spacing is 1.5 m); (3) excavation with equivalent reinforcement (the equivalent scale is about three times as cavern's span, according to

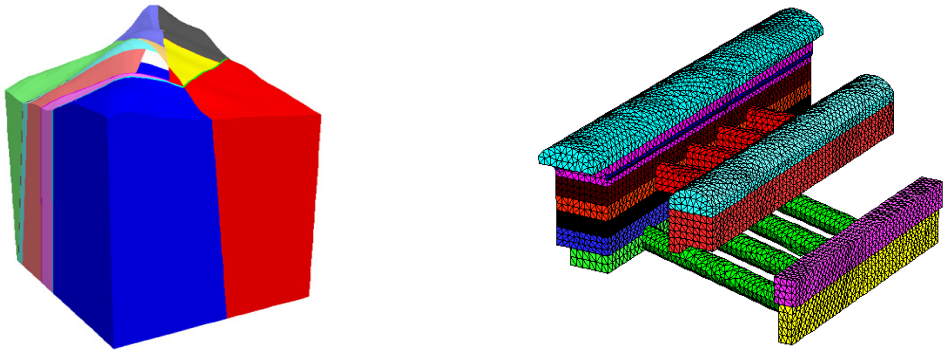

Fig. 13 Three-dimensional numerical model of Yi'meng hydro-power station

Table 3 Calculation parameters of numerical simulation

Classes	Density /(g/cm^3)	Elastic modulus /GPa	Poisson's ratio	Friction angle /(°)	Cohesion /MPa	Tensile strength /MPa
Rock mass	2.66	16.5	0.235	51	1.4	3.0
Virtual joint	-	-	-	45	1.2	2.5
Real joint	-	-	-	40.4	0.75	1.8
Bolt	-	90	-	-	-	170

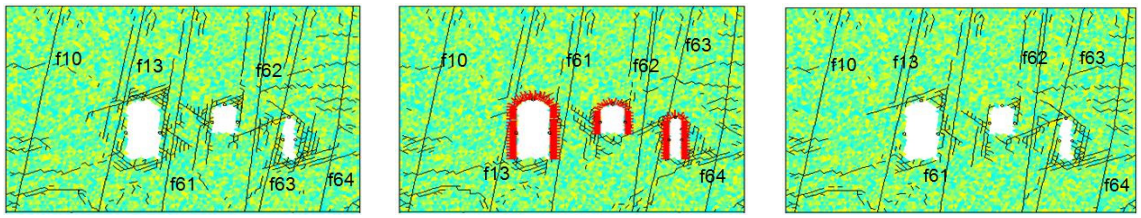

(a) Excavation without bolt (b) Excavation with full-length anchorage bolt (c) Excavation with equivalent reinforcement

Fig. 14 Crack expansion of surrounding rock masses with different reinforcement modes

Zhu and Zhang 1994). Vertical force is mainly the gravity of overlying rock masses. To improve the simulation efficiency, three main caverns' shapes are all simplified and the excavation uses one step. The calculation parameters are given in Table 3 and crack expansion results are shown in Fig. 14.

From Fig. 14, it can be observed that, after the excavation of three main caverns, expanded cracks' quantities and scales are quite large, greatly affect surrounding rock masses' safety and support is extremely urgent. Compare Figs. 14(b) and (c), whether the full-length anchorage bolt or equivalent reinforcement, they can both control the deformation of surrounding rock masses to a certain extent, and there are no obvious difference between them, crack expansion can be effectively suppressed, especially around the main workshop, its stability is improved obviously. Therefore, from the point of crack expansion, simulation on equivalent reinforcement can be in line well with that on real bolt reinforcement, the method of equivalent reinforcement has certain feasibility. At the same time, it has advantages of saving computation storage and improving calculation efficiency, because that there are no bolts' simulations in this method, and for this engineering simulation, the equivalent method can save the calculation time by 8.9% or so.

Take midpoints of arches and sidewalls as key points, their displacements are drawn in Fig. 15.

It shows up in Fig. 15, after the excavation without support, displacements of surrounding rock masses are greatly large, especially sidewalls' mid-parts of main workshop and tail room, the maximum displacement is up to 40.31 mm. It is mainly because those ratios of height to span

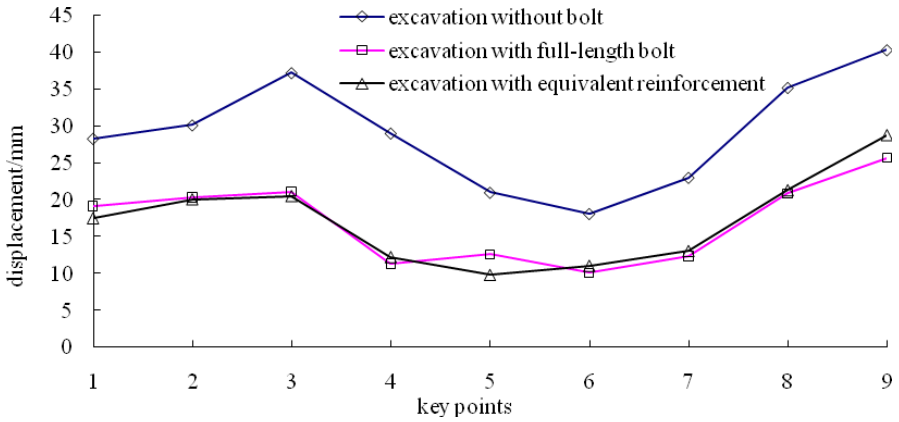

Fig. 15 Key points' displacements of Yi'meng hydro-power station

of these two caverns are too large, and also affected by faults; at the same time, one-off excavation has great disturbance on surrounding rock masses. As a result, such projects are suggested to adopt multi-steps excavation. Changes of three caverns' displacements show that, reinforcement modes including full-length anchorage bolt and equivalent reinforcement can control surrounding rock masses' deformation well. Compared to full-length anchorage bolt, the equivalent reinforcement effect is also obvious.

At present, reinforcement modes and their effects in DDARF are being explored, there is no doubt that equivalent reinforcement has provided a new train of thought. However, that the universality of formula, the rationality of parameters and so on have yet to be further verified.

5. Conclusions

In this contribution, new simulation algorithms of reinforcement modes in DDARF are proposed, in order to promote DDARF's application in rock engineering.

- Lining part can be set as one block or more, it usually has higher mechanical strength and must obey kinematic conditions. By means of AutoCAD, simulation on lining support is easy and feasible, which offers a new way for reinforcement in DDARF.
- Theoretical analyses and simulation algorithms of full-length anchorage bolt are given in details. This bolt offers axial force and shearing force in the meantime, its reinforcement effect is better than that of end-anchorage bolt. In view of the most common failure modes in rock engineering (bolt's broken and slippage failure), corresponding failure criterions are presented and numerical analysis consists with laboratory tests.
- Another reinforcement mode is equivalent support, it doesn't need any bolt elements and thus can save computer space. For a software having no strong methods to simulate bolts in rock engineering, equivalent support may become a wonderful idea.

Acknowledgments

The research described in this paper was financially supported by the National Natural Science Foundation of China (No. 51278287, No. 51609130 & No. 51509145), Program for Changjiang Scholars and Innovative Research Team in University of China (IRT13075), China Postdoctoral Science Foundation (No. 2016M592213 & No. 2015M582092) and Shandong Provincial Natural Science Foundation (ZR2016EEQ10 & ZR2015EQ005).

References

Chen, Y.J., Li, S.C., Zhu, W.S., Wang, W. and Wang, J. (2014), "A full-column shearing anchor bolt of discontinue deformation analysis for rock failure", *Rock Soil Mech.*, **35**(1), 293-297.

He, L., An, X.M. and Zhao, Z.Y. (2014), "Development of contact algorithm for three-dimensional numerical manifold method", *Int. J. Numer. Meth. Eng.*, **97**(6), 423-453.

Jiao, Y.Y., Zhang, X.L. and Zhao, J. (2012), "A two-dimensional DDA contact constitutive model for simulating rock fragmentation", *J. Eng. Mech.-ASCE*, **138**(2), 199-209.

Jiao, Y.Y., Zhang, H.Q., Tang, H.M., Zhang, X.L., Adoko, A.C. and Tian, H.N. (2014), "Simulating the process of reservoir-impoundment-induced landslide using the extended DDA method", *Eng. Geol.*, **182**,

37-48.
Ke, T.C. (1997), "Improved modeling of rock-bolting in DDA", *Proceedings of the 9th International Conference on Computer Methods and Advances in Geo-Mechanics*, Balkema, Rotterdam, The Netherlands, pp. 483-488.
Li, S.C., Chen, Y.J. and Zhu, W.S. (2013), "Failure and convergence criteria for bolts in DDARF", *Chin. J. Geotech. Eng.*, **35**(9), 1606-1611.
Li, S.C., Chen, Y.J. and Zhu, W.S. (2014), "Secondary development of elastic brittle constitutive model of discontinuous deformation analysis for rock failure", *Rock Soil Mech.*, **35**(8), 2144-2149.
Ma, G.W., An, X.M. and He, L. (2010), "The numerical manifold method: a review", *Int. J. Comp. Meth.*, **7**(1), 1-32.
Mohammadi, M. and Tavakoli, H. (2015), "Comparing the generalized Hoek-Brown and Mohr-Coulomb failure criteria for stress analysis on the rocks failure plane", *Geomech. Eng., Int. J.*, **9**(1), 115-124.
Ngoc, A.D., Pierpaolo, O., Daniel, D., Croce, A., Irini, D.M. and Locatelli, L. (2014), "Stress and strain state in the segmental linings during mechanized tunnelling", *Geomech. Eng., Int. J.*, **7**(1), 75-85.
Nikolic, M., Lbrahimbegovic, A. and Miscevic, P. (2015), "Brittle and ductile failure of rocks: Embedded discontinuity approach for representing mode I and mode II failure mechanisms", *Int. J. Numer. Meth. Eng.*, **102**(8), 1507-1526.
Noel, F., Leon, J.C. and Trompette, P. (1995), "A new approach to free-form surface mesh control in a CAD environment", *Int. J. Numer. Meth. Eng.*, **38**(18), 3121-3142.
Shi, G.H. (1988), "Discontinuous deformation analysis-a new numerical model for the statics and dynamics of block system", Ph.D. Dissertation; University of California, Berkeley, CA, USA.
Shi, G.H. (1993), *Block System Modeling By Discontinuous Deformation Analysis*, Computational Mechanics Publications, Southampton, UK & Boston, USA.
Shi, G.H. (1999), "Applications of discontinuous deformation analysis and manifold method", *Proceedings of the 3rd International Conference on DDA*, CO, USA.
Tateki, I., Kenjiro, T. and Takashi, K. (2006), "Failure analysis of quasi-brittle materials involving multiple mechanisms on fractured surfaces", *Int. J. Numer. Meth. Eng.*, **67**(7), 960-988.
Wu, Y.M. (2003), "Research on three-dimensional discontinuous deformation analysis method for jointed rock mass and its application", Ph.D. Dissertation; Wuhan university, Wuhan, China, April.
Zhang, X.L. (2007), "Study on numerical methods for modeling failure process of semi-continuous jointed rock mass", Ph.D. Dissertation; Institute of Rock and Soil Mechanics, Chinese Academy of Sciences, Wuhan, China.
Zhao, T.B. (2009), "Rock creep properties test in deep mine and deformation mechanism of anchored surrounding rock", Ph.D. Dissertation; Shandong University of Science and Technology, Qingdao, China.
Zheng, C.M. (2010), "Study on hydro-mechanical coupling of fractured rock mass based on DDA", Ph.D. Dissertation; Shandong university, Jinan, China.
Zhu, W.S. and Zhang, Y. (1994), "Effect of supporting rocks by bolts and its application to high slope of Three Gorges flight lock", *Proceeding of International Symposium on Anchoring and Grouting Techniques*, Guangzhou, China, December.
Zhu, W.S., Chen, Y.J., Li, S.C., Yin, F.Q., Yu, S. and Li, Y. (2014), "Rock failure and its jointed surrounding rocks: A multi-scale grid meshing method for DDARF", *Tunn. Undergr. Sp. Tech.*, **43**, 370-376.

CC